




Polyoxometalate tri-supported transition metal complexes containing mixed-valent transition metal ions

Li-Wei Fu, Li-Na Xiao, Hai-Yang Guo, Yang-Yang Hu, Lan-Lan Guo, Miao Yu, Xiao-Bing Cui & Ji-Qing Xu

To cite this article: Li-Wei Fu, Li-Na Xiao, Hai-Yang Guo, Yang-Yang Hu, Lan-Lan Guo, Miao Yu, Xiao-Bing Cui & Ji-Qing Xu (2015) Polyoxometalate tri-supported transition metal complexes containing mixed-valent transition metal ions, Journal of Coordination Chemistry, 68:21, 3814-3824, DOI: [10.1080/00958972.2015.1086484](https://doi.org/10.1080/00958972.2015.1086484)

To link to this article: <http://dx.doi.org/10.1080/00958972.2015.1086484>

 View supplementary material 

 Accepted author version posted online: 26 Aug 2015.
Published online: 25 Sep 2015.

 Submit your article to this journal 

 Article views: 59

 View related articles 

 View Crossmark data 

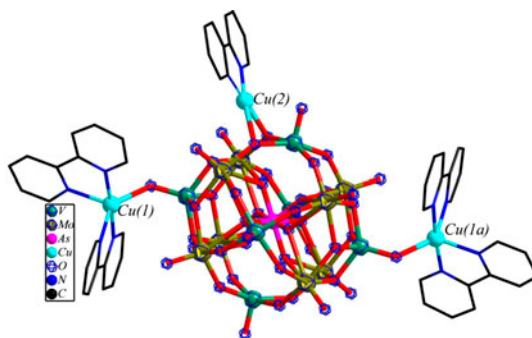
Polyoxometalate tri-supported transition metal complexes containing mixed-valent transition metal ions

LI-WEI FU[†], LI-NA XIAO[‡], HAI-YANG GUO[†], YANG-YANG HU[†], LAN-LAN GUO[†],
MIAO YU[†], XIAO-BING CUI^{*†} and JI-QING XU[†]

[†]State Key Laboratory of Inorganic Synthesis and Preparative Chemistry, Department of Chemistry, College of Chemistry, Jilin University, Changchun, China

[‡]Department of Chemistry, Zhoukou Normal University, Zhoukou, China

(Received 5 May 2015; accepted 6 August 2015)



Three compounds, $[\text{AsMo}_8\text{V}_6\text{O}_{42}][\text{Cu}(2,2'\text{-bpy})_2][\text{Cu}(2,2'\text{-bpy})]\cdot 4\text{H}_2\text{O}$ (**1**), $[\text{PMo}_8\text{V}_6\text{O}_{42}][\text{Cu}(2,2'\text{-bpy})_2][\text{Cu}(2,2'\text{-bpy})]\cdot 3\text{H}_2\text{O}$ (**2**) and $[\text{PMo}_8\text{V}_6\text{O}_{42}][\text{Cu}(2,2'\text{-bpy})_2][\text{Cu}(2,2'\text{-bpy})]\cdot 3.5\text{H}_2\text{O}$ (**3**), have been synthesized under hydrothermal conditions and characterized by IR, UV–vis, XRD, TG, elemental analysis, and X-ray diffraction analysis. Single-crystal X-ray structure analysis reveals that **1** and **2** are isostructural and isomorphous, whereas **2** and **3** are polymorphs. Polymorphs of **1** have not been synthesized yet. The mixed-valent transition metal ion in **1–3** has been further confirmed by TG analyses. Catalytic properties of **1** and **2** have also been studied.

Keywords: Polyoxometalates; Supported; Hydrothermal synthesis; Keggin; Hydrogen bonds

Polyoxometalates (POMs) constitute a unique class of inorganic compounds due to their structural variety and interesting properties in fields such as catalysis, medicine, and materials science [1]. This class of metal–oxygen clusters is formed by early transition metals of groups V and VI (V, Nb, Ta, Mo, and W) in their highest oxidation states (e.g. V^{5+} and W^{6+}) [2]. The existence of POMs has been known for almost 200 years, but the first

*Corresponding author. Email: cuixb@mail.jlu.edu.cn

structural details were only revealed in the last century [3, 4]; the number of POMs developed at an exponential rate.

Modification of the surface of the POMs has attracted much attention because of their intriguing structural versatility and potential applications in molecular devices, biochemistry, and catalysis [5, 6]. Capped POMs and POM-supported metal complexes have been regarded as two important families, which have become of increasing interest and relevance due to their topological and electronic versatility [7–15].

The Keggin POM is a valuable building block since it can be directly used to prepare materials where the structural integrity of the Keggin POM can be maintained throughout the construction processes (although with $(VO)^{2+}$ addition or metal exchange). A large number of Keggin POM-supported metal complexes have been synthesized, including Keggin POM mono- [16–22], bi- [23, 24] tri- [25], tetra- [24, 26, 27], and penta- [28] supported transition metal complexes. In Keggin POM-supported metal complexes, linking modes of transition metal complexes with the central cluster can be divided into three situations: (i) terminal-oxygen of the cluster [16, 17, 20–24], (ii) bridging-oxygen of the cluster [19, 25], and (iii) both terminal- and bridging-oxygens of the cluster [18, 26–28].

Our group has focused on POM-supported transition metal complexes for years. As continuing work in this system, in this paper we report the syntheses, structures, and properties of three Keggin POM-supported transition metal complexes formed via both terminal- and bridging-oxygens, formulated as $[AsMo_8V_6O_{42}][Cu(2,2'-bpy)_2][Cu(2,2'-bpy)] \cdot 4H_2O$ (**1**), $[PMo_8V_6O_{42}][Cu(2,2'-bpy)_2][Cu(2,2'-bpy)] \cdot 3H_2O$ (**2**) and $[PMo_8V_6O_{42}][Cu(2,2'-bpy)_2][Cu(2,2'-bpy)] \cdot 3.5H_2O$ (**3**). Compounds **2** and **3** are polymorphs. Polymorphism, defined as the phenomenon of a chemical species having more than one crystal form [29, 30], attracts attention because different forms may result in difference in terms of structures and physical and chemical properties. Several polymorphs based on different POMs have been reported [31–36]. Compounds **2** and **3** are two new examples of polymorphs based on Mo-V POMs.

2. Experimental

2.1. General procedures

All chemicals used were of reagent grade without purification. C, H, and N elemental analyses were carried out on a Perkin-Elmer 2400 CHN elemental analyzer. P, As, and metal contents were determined by inductively coupled plasma (ICP) analysis on a Perkin-Elmer Optima 3300DV ICP spectrometer. Infrared spectra were recorded as KBr pellets on a Perkin-Elmer SPECTRUM ONE FTIR spectrometer. XPS analyses were performed on a Thermo ESCALAB 250 spectrometer with a Mg-K α (1253.6 eV) achromatic X-ray source. UV–vis spectra of DMSO-saturated solutions of **1–3** were recorded on a Shimadzu UV3100 spectrophotometer. Small-angle X-ray diffraction (XRD) patterns were obtained on a Siemens D5005 diffractometer using Cu K α radiation. TG curves were performed on a Perkin-Elmer TGA-7000 thermogravimetric analyzer in flowing N₂ with a temperature ramp rate of 10 °C min⁻¹.

2.2. Preparation

2.2.1. Preparation of $[\text{AsMo}_8\text{V}_6\text{O}_{42}][\text{Cu}(2,2'\text{-bpy})_2]_2[\text{Cu}(2,2'\text{-bpy})]\cdot 4\text{H}_2\text{O}$ (1). Compound **1** was synthesized hydrothermally from a mixture of $(\text{NH}_4)_6\text{Mo}_7\text{O}_{24}\cdot 4\text{H}_2\text{O}$ (0.6 g, 0.49 mmol), $\text{H}_2\text{C}_2\text{O}_4\cdot 2\text{H}_2\text{O}$ (0.259 g, 2.05 mmol), $\text{Na}_3\text{AsO}_4\cdot 12\text{H}_2\text{O}$ (0.284 g, 1.34 mmol), NH_4VO_3 (0.233 g, 1.99 mmol), $\text{CuCl}_2\cdot 2\text{H}_2\text{O}$ (0.352 g, 2.06 mmol), 2,2'-bpy (0.162 g, 1.04 mmol), and distilled water (25 mL). The pH of the mixture was 5 after being stirred for 2 h, and then the resulting suspension was transferred to a 45-mL Teflon-lined autoclave. The mixture was heated under autogenous pressure at 160 °C for 5 days and then left to cool to room temperature. Dark block crystals could be isolated in 63% yield (based on Mo). Elemental analyses (%) Calcd: C, 20.97; H, 1.69; N, 4.89; As, 2.62; Mo, 26.80; V, 10.67; Cu, 6.66. Found: C, 20.75; H, 1.90; N, 4.61; As, 2.52; Mo, 26.47; V, 10.49; Cu, 6.39. FT-IR (KBr, cm^{-1}): 1620, 1597, 1490, 1469, 1443, 1311, 1250, 1224, 1171, 1156, 1103, 1033, 1016, 971, 955, 940, 907, 898, 871, 850, 807, 773, 759, 731, 669, 606, 528, 494, 464, 436, 380.

2.2.2. Preparation of $[\text{PMo}_8\text{V}_6\text{O}_{42}][\text{Cu}(2,2'\text{-bpy})_2]_2[\text{Cu}(2,2'\text{-bpy})]\cdot 3\text{H}_2\text{O}$ (2). Compound **2** was synthesized hydrothermally by reacting $(\text{NH}_4)_3\text{PMo}_{12}\text{O}_{40}\cdot x\text{H}_2\text{O}$ (FW \approx 1876.34, 0.499 g, 0.26 mmol), $\text{H}_2\text{C}_2\text{O}_4\cdot 2\text{H}_2\text{O}$ (0.253 g, 2.01 mmol), NH_4VO_3 (0.235 g, 2.01 mmol), $\text{Cu}(\text{NO}_3)_2\cdot 3\text{H}_2\text{O}$ (0.497 g, 2.06 mmol), 1,4-diazabicyclo[2,2,2]octane (0.232 g, 1.05 mmol), 2,2'-bpy (0.154 g, 0.99 mmol), and distilled water (25 mL) in a 45-mL Teflon-lined autoclave. The pH of the mixture was adjusted to 5 with $\text{NH}_3\cdot \text{H}_2\text{O}$ solution. The mixture was heated under autogenous pressure at 160 °C for 5 days and then left to cool to room temperature. Dark block crystals could be isolated in 57% yield (based on Mo). Elemental analyses (%) Calcd: C, 21.43; H, 1.65; N, 5.00; P, 1.11; Mo, 27.39; V, 10.91; Cu, 6.80. Found: C, 21.05; H, 1.85; N, 4.87; P, 1.11; Mo, 26.84; V, 10.72; Cu, 6.69. FT-IR (KBr, cm^{-1}): 1653, 1620, 1598, 1491, 1470, 1444, 1312, 1250, 1171, 1156, 1106, 1052, 1034, 1018, 963, 937, 818, 773, 730, 664, 609, 572, 541, 470, 420, 389, 321.

2.2.3. Preparation of $[\text{PMo}_8\text{V}_6\text{O}_{42}][\text{Cu}(2,2'\text{-bpy})_2]_2[\text{Cu}(2,2'\text{-bpy})]\cdot 3.5\text{H}_2\text{O}$ (3). Compound **3** was synthesized hydrothermally by reacting $(\text{NH}_4)_3\text{PMo}_{12}\text{O}_{40}\cdot x\text{H}_2\text{O}$ (FW \approx 1876.34, 0.501 g, 0.27 mmol), $\text{H}_2\text{C}_2\text{O}_4\cdot 2\text{H}_2\text{O}$ (0.253 g, 2.01 mmol), NH_4VO_3 (0.234 g, 2.0 mmol), $\text{Cu}(\text{NO}_3)_2\cdot 3\text{H}_2\text{O}$ (0.495 g, 2.05 mmol), 2-aminopyridine (0.125 g, 1.33 mmol), 2,2'-bpy (0.155 g, 0.99 mmol), and distilled water (25 mL) in a 45-mL Teflon-lined autoclave. The pH of the mixture was adjusted to 4 with NH_3 solution. The mixture was heated under autogenous pressure at 160 °C for 5 days and then left to cool to room temperature. Dark block crystals could be isolated in 52% yield (based on Mo). Elemental analyses (%) Calcd: C, 21.37; H, 1.69; N, 4.98; P, 1.10; Mo, 27.31; V, 10.87; Cu, 6.78. Found: C, 21.45; H, 1.66; N, 4.97; P, 1.01; Mo, 26.76; V, 10.93; Cu, 6.83. FT-IR (KBr, cm^{-1}): 1598, 1493, 1469, 1445, 1385, 1309, 1251, 1171, 1158, 1107, 1054, 1020, 986, 971, 947, 898, 873, 839, 775, 765, 728, 664, 637, 609, 538, 476, 417, 392, 315.

2.3. X-ray crystallographic analysis

All the reflection intensity data of **1–3** were collected on a Bruker Apex II diffractometer equipped with graphite monochromated Mo K_α ($\lambda = 0.71073 \text{ \AA}$) radiation at room

Table 1. Crystal data and structural refinements for **1–3**.

	1	2	3
Empirical formula	C ₅₀ H ₄₈ As ₁ Cu ₃ N ₁₀ O ₄₆ Mo ₈ V ₆	C ₅₀ H ₄₆ P ₁ Cu ₃ N ₁₀ O ₄₅ Mo ₈ V ₆	C ₅₀ H ₄₇ P ₁ Cu ₃ N ₁₀ O _{45.5} Mo ₈ V ₆
Formula weight	2863.71	2801.75	2810.73
Crystal system	Triclinic	Triclinic	Triclinic
Space group	<i>P</i> -1	<i>P</i> -1	<i>P</i> -1
<i>a</i> (Å)	11.658(1)	11.683(2)	14.707(3)
<i>b</i> (Å)	13.069(1)	13.132(3)	15.996(3)
<i>c</i> (Å)	13.351(1)	13.290(3)	19.181(4)
α (°)	87.020(1)	87.14(3)	68.88(3)
β (°)	79.057(1)	79.60(3)	67.58(3)
γ (°)	73.413(1)	72.72(3)	72.74(3)
Volume (Å ³)	1914.0(3)	1914.9(7)	3824(1)
<i>Z</i>	1	1	2
<i>D</i> _C (Mg m ⁻³)	2.484	2.435	2.440
μ (mm ⁻¹)	3.305	2.894	2.899
<i>F</i> (0 0 0)	1379	1357	2712
θ for data collection	1.85–25.00	3.04–27.48	3.01–25.00
Reflections collected	9817	18,701	27,759
Reflections unique	6646	8600	12,931
<i>R</i> (int)	0.0160	0.0367	0.0720
Completeness to θ	98.6	98.2	95.9
Parameters	571	571	1114
GOF on <i>F</i> ²	1.015	1.070	1.081
<i>R</i> ^a [<i>I</i> > 2 σ (<i>I</i>)]	<i>R</i> ₁ = 0.0997	<i>R</i> ₁ = 0.0688	<i>R</i> ₁ = 0.0875
<i>R</i> ^b (all data)	$\omega R_2 = 0.2183$	$\omega R_2 = 0.1725$	$\omega R_2 = 0.2598$

$$^a R_1 = \frac{\sum ||F_o| - |F_c||}{\sum |F_o|}$$

$$^b \omega R_2 = \left\{ \frac{\sum [w(F_o^2 - F_c^2)]^2}{\sum [w(F_o^2)]^2} \right\}^{\frac{1}{2}}$$

temperature. The structures of **1–3** were solved by direct methods and further refined using full-matrix least-squares on *F*² using the SHELXTL-97 crystallographic software package. Anisotropic thermal parameters were refined for all non-hydrogen atoms in **1–3**. All the hydrogens of ligands were placed in geometrically calculated positions and refined with fixed isotropic displacement parameters using a riding model except the lattice water molecules in **1–3**. A summary of the crystallographic data and structure refinements for **1–3** are given in table 1. CCDC: 1,061,363 for **1**, 1,061,364 for **2** and 1,061,365 for **3**.

3. Results and discussion

3.1. Syntheses

Only when the pH value was 5, and only when the pH was 4, we succeeded in synthesizing **2** and **3**. Parallel experiments with pH deviating from those pH values yielded very little target compound, nothing or some unidentified powders. The presence of H₂C₂O₄·2H₂O is important for preparations of **1–3**. It is not only a reducing agent for the reductions of Cu²⁺ to Cu⁺ and V⁵⁺ to V⁴⁺ but also an important reagent to control the final pH of reaction mixtures. We also tried to synthesize similar compounds to **1–3** by additions of other carboxylic acids such as isonicotinic acid, malonic acid, benzoic acid, and pyridinedicarboxylic acid, but these attempts were not successful.

3.2. Structure descriptions

3.2.1. Crystal structures of 1 and 2. The crystal structures of **1** and **2** are isomorphous and isostructural, belonging to the triclinic space group *P*-1. Here, **1** is described in detail as an example.

The asymmetric unit of **1** is composed of half a bi-capped pseudo-Keggin polyoxoanion $[\text{AsMo}_8\text{V}_6\text{O}_{42}]^{5-}$, a $[\text{Cu}(2,2'\text{-bpy})_2]^{2+}$, half a $[\text{Cu}(2,2'\text{-bpy})]^+$, and two water molecules. $[\text{AsMo}_8\text{V}_6\text{O}_{42}]^{5-}$ can be described as the well-known pseudo-Keggin core with two additional VO^{2+} units capping two opposite pits. As–O bond distances are 1.61(2)–1.72(3) Å. Mo–O bonds can be divided into three groups: Mo–O_c (O_c, central O atoms), 2.38(3)–2.48(2) Å; Mo–O_b (O_b, bridging O atoms), 1.77(1)–2.10(1) Å; Mo–O_t (O_t, terminal O atoms), 1.66(1)–1.68(1) Å. In addition, V–O distances can be divided into two groups: V–O_b (O_b, bridging O atoms), 1.92(2)–2.01(2) Å; V–O_t (O_t, terminal O atoms), 1.55(1)–1.57(1) Å. Bond valence sum (BVS) calculations for the molybdenum and vanadium of **1** were calculated using parameters given by Brown [37]. Results reveal that the oxidation state of the four independent molybdenum ions is +6, the oxidation state of one vanadium is +4 and the oxidation state of the other two vanadium ions is +5. Thus, the formula of the POM is $[\text{AsMo}^{\text{VI}}_8\text{V}^{\text{IV}}_4\text{V}^{\text{V}}_2\text{O}_{42}]^{5-}$.

The anion $[\text{AsMo}_8\text{V}_6\text{O}_{42}]^{5-}$ serves as a multidentate ligand coordinating to three copper ions. Copper ions in **1** could be grouped into two types: $[\text{Cu}(2,2'\text{-bpy})_2]^{2+}$ and $[\text{Cu}(2,2'\text{-bpy})]^+$. The Cu center of the former not only receives the contribution from a terminal oxygen from $[\text{AsMo}_8\text{V}_6\text{O}_{42}]^{5-}$ with a Cu–O distance of 2.02(1) Å but also receives contributions from four 2,2'-bpy nitrogens with Cu–N distances of 1.97(1)–2.09(1) Å. Thus, a square pyramidal coordination environment around copper is completed. The Cu center of the latter is coordinated by two nitrogens from a 2,2'-bpy with Cu–N distances of 1.89(3)–2.01(1) Å and two oxygens from $[\text{AsMo}_8\text{V}_6\text{O}_{42}]^{5-}$ with Cu–O distances of 2.18(2)–2.38(2) Å. Thus, the Cu center exhibits a square planar geometry. In other words, two different transition metal complexes are supported by $[\text{AsMo}_8\text{V}_6\text{O}_{42}]^{5-}$ via both terminal- and bridging-oxygens, forming a POM tri-supported transition metal unit $\{[\text{AsMo}_8\text{V}_6\text{O}_{42}]^{5-}[\text{Cu}(2,2'\text{-bpy})_2]_2[\text{Cu}(2,2'\text{-bpy})]\}$, as shown in figure 1. The valence of the copper ions can be further confirmed by BVS calculations using parameters given by Brown [37], which shows that

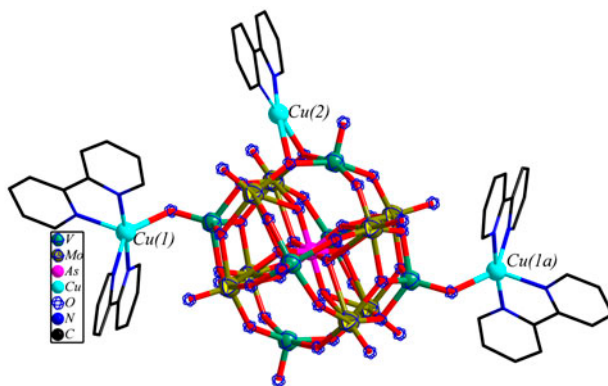


Figure 1. Ball-and-stick and wire representation of the POM supported transition metal complex in **1**.

the BVS values for the coppers in $[\text{Cu}(2,2'\text{-bpy})_2]^{2+}$ and $[\text{Cu}(2,2'\text{-bpy})]^+$ are 1.73 and 1.25, respectively.

In addition, **1** contains a binuclear water cluster $(\text{H}_2\text{O})_2$. The water cluster is formed by Ow(1) and Ow(1a, a: $1-x, 1-y, 1-z$) with a distance of 2.5298(2) Å. There are O–H...O hydrogen bonding interactions between oxygens of the water cluster and oxygens of $[\text{AsMo}_8\text{V}_6\text{O}_{42}]^{5-}$. O...O distances of hydrogen bonds are 2.7999(2)–2.8735(2) Å. Alternatively, each water cluster as a rod joins $[\text{AsMo}_8\text{V}_6\text{O}_{42}]^{5-}$ through hydrogen bonds into a supramolecular chain structure.

There exist $\pi \cdot \cdot \pi$ interactions between phenol rings of different 2,2'-bpy ligands with the interplanar distance of about 3.50 Å. There also is a C–H...O hydrogen bonding interaction between C(10) of 2,2'-bpy and O(23) of $[\text{AsMo}_8\text{V}_6\text{O}_{42}]^{5-}$ with a bond distance of 3.110(2) Å. Thus, a 3-D supramolecular structure is formed through O–H...O, $\pi \cdot \cdot \pi$ and C–H...O interactions.

Not only are **1** and **2** isomorphous and isostructural to each other, but also they are isostructural and isostructural to $[\text{Mo}_8\text{V}_7\text{O}_{42}][\text{Cu}(2,2'\text{-bpy})_2]_2[\text{Cu}(2,2'\text{-bpy})]\cdot 2\text{H}_2\text{O}$ we reported recently [38]; the main difference of the two and $[\text{Mo}_8\text{V}_7\text{O}_{42}][\text{Cu}(2,2'\text{-bpy})_2]_2[\text{Cu}(2,2'\text{-bpy})]\cdot 2\text{H}_2\text{O}$ is the heteroatom enclosed, it is As and P for **1** and **2**, but V for the compound reported. Compound **2** was almost identical to the compound we synthesized previously with only slight differences in the numbers of lattice water molecules [39].

3.2.2. Crystal structure of 3. X-ray diffraction analysis reveals that the asymmetric unit of **3** consists of a bi-capped Keggin polyoxoanion, two $[\text{Cu}(2,2'\text{-bpy})_2]^{2+}$ units, a $[\text{Cu}(2,2'\text{-bpy})]^+$, and three water molecules. $[\text{PMo}_8\text{V}_6\text{O}_{42}]^{5-}$ is very similar to $[\text{AsMo}_8\text{V}_6\text{O}_{42}]^{5-}$ in **1**, the main difference of the two is the central unit, a disordered AsO_4^{3-} cube in **1**, but an ordered PO_4^{3-} tetrahedron in **3**. P–O bond distances are 1.52(1)–1.56(1) Å. Mo–O and V–O distances are all comparable to those in **1**. The BVS model clearly indicates that all the eight molybdenum ions are in the +6 oxidation state, two vanadium ions are in the +5 oxidation state, and the remaining four vanadium ions are in the +4 oxidation state. Thus, the formula of the POM is $[\text{PMo}^{\text{VI}}_8\text{V}^{\text{IV}}_4\text{V}^{\text{V}}_2\text{O}_{42}]^{5-}$.

The role of the POM in **3** is similar to that of **1(2)**, serving as a multidentate ligand coordinating to three copper ions. Also, the transition metal complexes of **3** could be

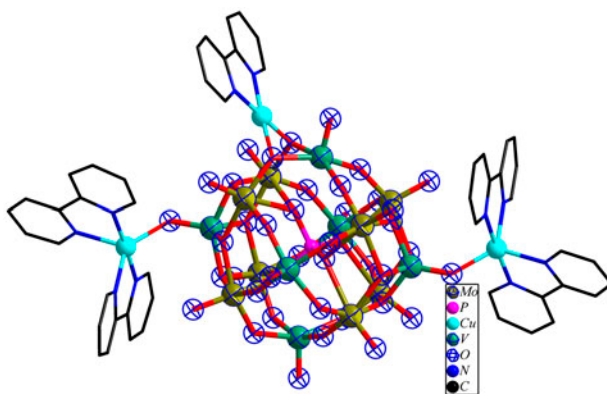


Figure 2. Ball-and-stick and wire representation of the POM supported transition metal complex in **2**.

grouped into two types: $[\text{Cu}(2,2'\text{-bpy})_2]^{2+}$ and $[\text{Cu}(2,2'\text{-bpy})]^{+}$. The Cu center of the former is similar to that of **1(2)** with square pyramidal geometry. The Cu of the latter is also similar to that of **1(2)**, displaying a square planar geometry.

The anion $[\text{PMo}_8\text{V}_6\text{O}_{42}]^{5-}$ also supports two different types of transition metal complexes: $[\text{Cu}(2,2'\text{-bpy})_2]^{2+}$ and $[\text{Cu}(2,2'\text{-bpy})]^{+}$ with Cu–O contacts via both terminal- and bridging-oxygens, forming a POM tri-supported transition metal complex containing mixed-valent transition metal ions $\{[\text{PMo}_8\text{V}_6\text{O}_{42}][\text{Cu}(2,2'\text{-bpy})_2]_2[\text{Cu}(2,2'\text{-bpy})]\}$ (figure 2). The valence of copper ions can be further confirmed by BVS calculations [37]. The oxidation state of the copper ion in $[\text{Cu}(2,2'\text{-bpy})_2]^{2+}$ is +2 and the oxidation state of the copper ion in $[\text{Cu}(2,2'\text{-bpy})]^{+}$ is +1.

There exist $\pi \cdot \pi$ interactions between phenol rings of 2,2'-bpy ligands with the interplanar distance of about 3.50 Å. There also exist C–H \cdots O hydrogen bonding interactions between C(30) of 2,2'-bpy and O(22) of $[\text{PMo}_8\text{V}_6\text{O}_{42}]^{5-}$ with a bond distance of 3.0946(9) Å.

Compound **3** is also similar to the compound we synthesized previously with only slight differences in the numbers of lattice water molecules [39]. However, **2** and **3** are not isomorphous and isostructural to each other, but polymorphs. Therefore, the two compounds we reported previously are also polymorphs [39]. Up to now, only the POM with P as heteroatom was found to have different polymorphs; however, the POM with As or V as heteroatom were not found to have polymorphs.

3.3. Properties

3.3.1. XRD analysis. The X-ray powder diffraction patterns of **1–3** are in agreement with the simulated XRD patterns (figure S1), confirming the phase purity of **1–3**. The differences in reflection intensities are probably due to preferential orientations in the powder samples of **1–3**.

3.3.2. UV–Vis spectroscopy. UV–vis spectra of **1–3**, from 250 to 600 nm, are presented in figure S2. The UV–vis spectrum of **1** displays an intense sharp absorption at 254 nm with two shoulder peaks at 287 and 312 nm assigned to O \rightarrow Mo, O \rightarrow V charge transfers and $n \rightarrow \pi^*$ transitions of 2,2'-bpy in **1**. The UV–vis spectra of **2** and **3** exhibit very similar intense sharp absorptions and shoulders to **1** centered at 255, 288, 312 and 255, 286, 312 nm, respectively, which should be ascribed to transfer bands of O \rightarrow Mo, O \rightarrow V and $n \rightarrow \pi^*$ transitions of organic ligands in **2** and **3**.

3.3.3. XPS spectra. The XPS spectra in the V 2P region present four peaks at 524.2, 523.1, 517.1, and 515.8 eV for **1** (figure S3), 524.7, 523.1, 517.5, and 516.0 eV (figure S3) for **2**, and 524.8, 523.5, 517.3, and 516.0 eV for **3** (figure S3), which should be attributed to mixture of V^{5+} and V^{4+} in **1–3**, respectively. The XPS spectra in the Mo 3-D region show two peaks at 235.6 and 232.6 eV for **1** (figure S4), 235.4 and 232.4 eV for **2** (figure S4), and 235.8 and 232.5 eV for **3** (figure S4), which should be owing to Mo^{6+} in **1–3**. It should be noted that the XPS spectra for **1–3** are very similar to each other. The XPS analyses are in agreement with the BVS values.

3.3.4. TG analysis. The TG curve of **1** can be divided into three stages (figure S5). The first stage is from room temperature to 277 °C with a weight loss of 2.57%, which is consistent with the release of the crystallization water molecules in **1** (calculated: 2.51%). The second stage is from 277 to 422 °C with a weight loss of 5.73%, which is due to release of the 2,2'-bpy in $[\text{Cu}(2,2'\text{-bpy})]^+$ in **1**. The third stage is from 422 to 720 °C with a weight loss of 21.60%, which corresponds to combustion of 2,2'-bpy in $[\text{Cu}(2,2'\text{-bpy})_2]^{2+}$ in **1**. The total weight of the TG curve is 29.89%, which is consistent with the calculated result 29.79%. The TG analysis of **1** further demonstrated that there are two different kinds of transition metal complexes containing transition metal ions with different valences. The interaction between copper and the 2,2'-bpy ligand is weak for copper ion in $[\text{Cu}(2,2'\text{-bpy})]^+$; thus, the 2,2'-bpy ligand in $[\text{Cu}(2,2'\text{-bpy})]^+$ was released first. The interaction between copper and the 2,2'-bpy ligand is strong for the high-valent copper ion in $[\text{Cu}(2,2'\text{-bpy})_2]^{2+}$; thus, the 2,2'-bpy ligand in $[\text{Cu}(2,2'\text{-bpy})_2]^{2+}$ was released finally.

The TG analysis of **2** from 35 to 800 °C is similar to that of **1** and can also be divided into three stages. The first stage is from room temperature to 333 °C with a weight loss of 2.21%, which is ascribed to release of lattice water molecules (calculated: 1.93%). The second stage is from 333 to 456 °C with a weight loss of 5.97% for **2**, which is associated with release of 2,2'-bpy in $[\text{Cu}(2,2'\text{-bpy})]^+$ (calculated: 5.57%). The third stage is from 456 to 738 °C with a weight loss of 22.53%, which can be owing to the combustion of the 2,2'-bpy ligand in $[\text{Cu}(2,2'\text{-bpy})_2]^{2+}$ (calculated: 22.30%). Three stages were also observed in the TG curve of **3**. The first stage is from room temperature to 315 °C with a weight loss of 2.11%, consistent with the release of lattice water molecules (calculated: 2.24%). However, only the first stage of the TG curve of **3** is similar to those of **1** and **2**. The second stage is from 315 to 451 °C with a weight loss of 8.97%, due to release of 2,2'-bpy in $[\text{Cu}(2,2'\text{-bpy})]^+$ and part of the 2,2'-bpy ligand in $[\text{Cu}(2,2'\text{-bpy})_2]^{2+}$. The third stage is from 451 to 683 °C with a weight loss of 18.53% for **3**, which corresponds to combustion of part of the 2,2'-bpy in $[\text{Cu}(2,2'\text{-bpy})_2]^{2+}$. However, the total weight of the TG curve of **3** is 28.98%, which is consistent with the calculated result 30.03%.

The TG analysis of **2** and **3** further demonstrated that there are two different kinds of transition metal complexes containing transition metal ions with different valences just like that of **1**.

3.3.5. Catalytic properties. The epoxidation of styrene to styrene oxide with aqueous tert-butyl hydroperoxide (TBHP) using **1** or **2** as a catalyst was carried out in a batch reactor. In a typical run, the catalyst (**1** (10 mg, 3.5 μmol), **2** (10 mg, 3.6 μmol)), 0.114 mL (1 mmol) of styrene, and 1 mL of CH₃CN were added to a 10-mL two-neck flask equipped with a stirrer and a reflux condenser. The mixture was heated to 80 °C and then 2 mmol of TBHP was injected into the solution to start the reaction. The liquid organic products were

Table 2. Catalytic activity and product distribution.

Catalysts	Styrene conversion (%)	Product selectivity (%)	
		Styrene oxide	Benzaldehyde
Compound 1	93.6	72.5	27.5
Compound 2	90	87.2	12.8

quantified using a gas chromatograph (Shimadzu, GC-8A) equipped with a flame detector and an HP-5 capillary column and identified by comparison with authentic samples and GC-MS coupling. The activity of the reaction system to oxidize styrene to styrene oxide in the absence of the catalysts was determined. The result showed no conversion of the styrene after 8 h.

Table 2 shows the reaction results of TBHP oxidation of styrene with **1** and **2** at 80 °C. As expected, the two catalysts are active for the TBHP oxidation of styrene. Compound **1** shows activity with 93.6% conversion and 72.5% selectivity to styrene oxide after 8 h. Compound **2** shows lower activity with 90% conversion of styrene and 87.2% selectivity to styrene oxide.

We have carried out identical catalytic experiments previously with some As-V cluster compounds as catalysts, and from those experiments, we found that transition metal elements are essential for catalytic properties of catalysts used and the structures of catalysts used also affect their catalytic activities [40]. Du *et al.*, Moradi-Shoeili *et al.*, Heikkilä *et al.*, and Li have demonstrated that molybdenum clusters exhibit high catalytic activity and stability for olefin epoxidation [41–44]. Both **1** and **2** contain molybdenums and transition metal elements, so perhaps both molybdenum and transition metal ions are important for the catalytic properties of the two compounds.

The conventional organic oxidants (TBHP) produce copious amounts of environmentally undesirable waste [45]. From the sustainable and green chemistry point of view, the use of molecular oxygen or H₂O₂ for the oxidation of olefins is a very attractive and desirable idea [46]. Therefore, H₂O₂ was used as the oxidant for the epoxidation of cyclooctene to cyclooctene oxide.

Epoxidation of cyclooctene to cyclooctene oxide with aqueous H₂O₂ solution using **2** as catalyst was carried out in a batch reactor. In a typical run, the catalyst (**2** (10 mg, 3.6 μmol)), 2 mL of acetonitrile, and 1 mmol of cyclooctene were added to a 10-mL two-neck flask equipped with a stirrer and a reflux condenser. The mixture was heated to 80 °C and then 2 mmol of H₂O₂ was injected into the solution to start the reaction. The liquid organic products were quantified using a gas chromatograph (Shimadzu, GC-8A) equipped with a flame detector and an HP-5 capillary column and identified by comparison with authentic samples and GC-MS coupling. The activity of the reaction system to oxidize cyclooctene to cyclooctene oxide in the absence of the catalysts was zero after 9 h.

As expected, **2** is active for H₂O₂ oxidation of cyclooctene. Compound **2** shows 52.26% conversion and 100% selectivity to cyclooctene oxide after 9 h. It should be noted that the reaction temperature is very important for the H₂O₂ oxidation of cyclooctene. We have also carried out the same catalytic reaction except that the reaction temperature is 60 °C with only 2.61% conversion and 100% selectivity to cyclooctene oxide after 9 h.

4. Conclusion

We have described three new Mo-V-O compounds synthesized by hydrothermal method. Compounds **1** and **2** are bi-capped pseudo-Keggin polyoxoanion, [Cu(2,2'-bpy)₂]²⁺ and [Cu(2,2'-bpy)]⁺ as well as water molecules, while **3** is composed of bi-capped Keggin polyoxoanion, [Cu(2,2'-bpy)₂]²⁺ and [Cu(2,2'-bpy)]⁺ as well as water molecules. Further research is underway to determine the rules of their synthesis and to explore their properties.

Acknowledgments

This work was supported by the National Natural Science Foundation of China (NSFC) [grant numbers 21003056 and 21501203] and the open project of State Key Laboratory of Inorganic Synthesis and Preparative Chemistry [grant number 2013-25].

Disclosure statement

No potential conflict of interest was reported by the authors.

Supplemental data

The supplemental data for this paper is available online at <http://dx.doi.org/10.1080/00958972.2015.1086484>.

References

- [1] M.T. Pope, A. Müller. *Polyoxometalates: From Platonic Solids to Anti-Retro Viral Activity*, Kluwer, Dordrecht, The Netherlands (1994).
- [2] M.T. Pope. *Heteropoly and Isopoly Oxometalates*, Springer-Verlag, Berlin (1983).
- [3] J.F. Keggin. *Nature*, **131**, 908 (1933).
- [4] J. Berzelius. *Ann. Phys.*, **6**, 369 (1826).
- [5] A. Proust, R. Thouvenot, P. Guozerh. *Chem. Commun.*, 1837 (2008).
- [6] Q. Li, Y.G. Wei, J. Hao, Y.L. Zhu, L.S. Wang. *J. Am. Chem. Soc.*, **129**, 5810 (2007).
- [7] W.M. Bu, L. Ye, G.Y. Yang, J.S. Gao, Y.G. Fan, M.C. Shao, J.Q. Xu. *Inorg. Chem. Commun.*, **4**, 1 (2001).
- [8] C. Lei, J.G. Mao, Y.Q. Sun, J.L. Song. *Inorg. Chem.*, **43**, 1964 (2004).
- [9] Z.G. Han, T. Chai, X.L. Zhai, J.Y. Wang, C.W. Hu. *Solid State Sci.*, **11**, 1998 (2009).
- [10] Z.M. Zhang, J. Liu, E.B. Wang, C. Qin, Y.G. Li, Y.F. Qi, X.L. Wang. *Dalton Trans.*, 463 (2008).
- [11] Z.M. Zhang, Y.F. Qi, E.B. Wang, Y.G. Li, H.Q. Tan. *Inorg. Chim. Acta*, **361**, 1979 (2008).
- [12] L.H. Bi, G.F. Hou, L.X. Wu, U. Kortz. *CrystEngComm*, **11**, 1532 (2009).
- [13] L.J. Dong, R.D. Huang, Y.G. Wei, W. Chu. *Inorg. Chem.*, **48**, 7528 (2009).
- [14] C.M. Liu, J.L. Luo, D.Q. Zhang, N.L. Wang, Z.J. Chen, D.B. Zhu. *Eur. J. Inorg. Chem.*, 4774 (2004).
- [15] C.M. Liu, D.Q. Zhang, M. Xiong, D.B. Zhu. *Chem. Commun.*, 1416 (2002).
- [16] Y. Xu, J.Q. Xu, K.L. Zhang, Y. Zhang, X.Z. You. *Chem. Commun.*, 153 (2000).
- [17] S. Reinoso, P. Vitoria, L. Felices, L. Lezama, J.M. Gutiérrez-Zorrilla. *Inorg. Chem.*, **45**, 108 (2006).
- [18] J.Y. Niu, Z.L. Wang, J.P. Wang. *Inorg. Chem. Commun.*, **6**, 1272 (2003).
- [19] Y. Lu, Y. Xu, E.B. Wang, J. Lü, C.W. Hu, L. Xu. *Cryst. Growth Des.*, **5**, 257 (2005).
- [20] J.W. Cui, X.B. Cui, H.H. Yu, J.Q. Xu, Z.H. Yi, W.J. Duan. *Inorg. Chim. Acta*, **361**, 2641 (2008).
- [21] J. Liu, J.N. Xu, Y.B. Liu, Y.K. Lu, J.F. Song, X. Zhang, X.B. Cui, J.Q. Xu, T.G. Wang. *J. Solid State Chem.*, **180**, 3456 (2007).
- [22] Y. Wang, L.N. Xiao, H. Ding, F.Q. Wu, L. Ye, T.G. Wang, S.Y. Shi, X.B. Cui, J.Q. Xu, D.F. Zheng. *Inorg. Chem. Commun.*, **13**, 1184 (2010).
- [23] C.M. Liu, D.Q. Zhang, D.B. Zhu. *Cryst. Growth Des.*, **3**, 363 (2003).
- [24] M. Yuan, Y.G. Li, E.B. Wang, C.G. Tian, L. Wang, C.W. Hu, N.H. Hu, H.Q. Jia. *Inorg. Chem.*, **42**, 3670 (2003).
- [25] Y.K. Lu, X.B. Cui, Y.B. Liu, Q.F. Yang, S.Y. Shi, J.Q. Xu, T.G. Wang. *J. Solid State Chem.*, **182**, 690 (2009).
- [26] G.Y. Luan, Y.G. Li, S.T. Wang, E.B. Wang, Z.B. Han, C.W. Hu, N.H. Hu, H.Q. Jia. *J. Chem. Soc., Dalton Trans.*, 233 (2003).
- [27] S. Reinoso, P. Vitoria, L. Lezama, A. Luque, J.M. Gutiérrez-Zorrilla. *Inorg. Chem.*, **42**, 3709 (2003).
- [28] Z.G. Han, Y.L. Zhao, J. Peng, H.Y. Ma, Q. Liu, E.B. Wang, N.H. Hu, H.Q. Jia. *Eur. J. Inorg. Chem.*, 264 (2005).
- [29] D. Fox, M.M. Labes, A. Weissberger. *Polymorphism in Physics and Chemistry of the Organic Solid State*, Wiley Interscience, New York (1965).

- [30] G.R. Desiraju. *Conformational Polymorphism in Organic Solid State Chemistry*, Elsevier, Amsterdam (1987).
- [31] P. Roman, A. Luque, A. Aranzabe, J.M. Gutierrez-Zorrilla. *Polyhedron*, **11**, 2027 (1992).
- [32] J. Hao, L. Ruhlmann, Y.L. Zhu, Q. Li, Y.G. Wei. *Inorg. Chem.*, **46**, 4960 (2007).
- [33] J.H. Son, Y.U. Kwon. *Inorg. Chim. Acta*, **358**, 310 (2005).
- [34] X. Liu, H.Y. An, Z.F. Chen, H. Zhang, Y. Hu, G.B. Zhu, Y.V. Geletii, C.L. Hill. *Eur. J. Inorg. Chem.*, 1827 (2013).
- [35] H.Y. Liu, B. Liu, J. Yang, Y.Y. Liu, J.F. Ma, H. Wu. *Dalton Trans.*, **40**, 9872 (2011).
- [36] B. Nohra, H.E. Moll, L.M.R. Albelo, P. Mialane, J. Marrot, C. Mellot-Draznieks, M. O'Keefe, R.N. Biboum, J. Lemaire, B. Keita, L. Nadjó, A. Dolbecq. *J. Am. Chem. Soc.*, **133**, 13363 (2011).
- [37] I.D. Brown. In *Structure and Bonding in Crystals*, M. O'Keefe, A. Navrotsky (Eds), Vol. 2, pp. 1–29, Academic Press, New York (1981).
- [38] L.N. Xiao, Y. Wang, Y. Chen, Y. Peng, G.D. Li, X.B. Cui, S.Y. Shi, T.G. Wang, Z.M. Gao, J.Q. Xu. *Inorg. Chem. Commun.*, **13**, 1217 (2010).
- [39] J.W. Cui, X.B. Cui, J.N. Xu, H.H. Yu, J.Q. Xu, W.J. Duan, T.G. Wang. *J. Mol. Struct.*, **891**, 35 (2008).
- [40] H.Y. Guo, Z.F. Li, D.C. Zhao, Y.Y. Hu, L.N. Xiao, X.B. Cui, J.Q. Guan, J.Q. Xu. *CrystEngComm.*, **16**, 2251 (2014).
- [41] J. Du, J.H. Yu, J.Y. Tang, J. Wang, W.X. Zhang, W.R. Thiel, M.J. Jia. *Eur. J. Inorg. Chem.*, 2361 (2011).
- [42] Z. Moradi-Shoeili, M. Zare, M. Bagherzadeh, M. Kubicki, D.M. Boghaei. *J. Coord. Chem.*, **68**, 548 (2015).
- [43] T. Heikkilä, R. Sillanpää, A. Lehtonen. *J. Coord. Chem.*, **67**, 1863 (2014).
- [44] A.M. Li. *J. Coord. Chem.*, **67**, 1022 (2014).
- [45] S. Khare, R. Chochare. *J. Mol. Catal. A: Chem.*, **344**, 83 (2011).
- [46] Y. Yang, Y. Zhang, S.J. Hao, Q.B. Kan. *Chem. Eng. J.*, **171**, 1356 (2011).